Synthesis and Photophysics of a Copper-Porphyrin−Styrene−C_{60} Hybrid†

Dirk M. Guldi*,‡

Radiation Laboratory, University of Notre Dame, Notre Dame, Indiana 46556

Berthold Nuber, Paul J. Bracher, Christopher A. Alabi, Shaun MacMahon, Jonathan W. Kukol, Stephen R. Wilson, and David I. Schuster*,§

Department of Chemistry, New York University, New York, New York 10003

Received: July 9, 2002; In Final Form: September 24, 2002

A new conjugated porphyrin−fullerene dyad featuring a styrene linkage has been prepared in 11% overall yield from previously synthesized starting materials. In contrast to the singlet and triplet excited states commonly observed in analogous systems with zinc and free base porphyrins, the present investigation involves doublet and quartet ground and excited states. The photophysical pathways in the present system include intramolecular electron and energy transfer events, whose outcome depends predominantly on the solvent polarity.

Introduction

One of the ultimate goals of molecular electronics is the rational design of donor−acceptor ensembles capable of light-induced charge-separation over long distances on the molecular scale. Toward these ends, ultrafast charge-transfer systems will likely figure prominently in proposed photodriven molecular-scale rectifiers and emerging technologies that focus on light-modulated data storage and retrieval.

There has been considerable sustained interest in donor−acceptor systems in which fullerenes serve as electron and energy acceptors upon photoexcitation.[1−3] While a large variety of such systems have been synthesized and subjected to photophysical investigation, the greatest attention has been paid to systems in which porphyrins are linked to [60]fullerene (C_{60}) by a variety of flexible, rigid, and semirigid linkers.[4,5]

Fullerenes and porphyrins are molecular architectures ideally suited for devising integrated, multicomponent model systems to transmit and process solar energy. The implementation of C_{60} as a three-dimensional electron acceptor holds great expectations on account of its small reorganization energy in electron-transfer reactions, which has exerted a noteworthy impact on the development of fullerene-based materials for applications involving light-induced charge-separation.[1,2,6−10] As a result of van der Waals attraction between porphyrins and fullerenes, dyads tend to adopt conformations where these moieties achieve close spatial proximity if allowed by the molecular topology of the system.[11,12] Several groups have successfully constructed doubly-linked hybrids in which the two chromophores are forced into close proximity, such that the distance between the center of the porphyrin and the center of the fullerene sphere is on the order of 6.5−7.0 Å.[13−15] Photoinduced electron transfer (ET) in such systems is extremely fast, occurring in the short picosecond time domain, usually to the exclusion of intramolecular energy transfer (EnT).[13−16] In systems where the two moieties are held further apart, both ET and EnT occur, with the polarity of the solvent being a crucial parameter regulating the competition between the two processes.[17,18]

We are interested in how a conjugated π-linker affects the nature and dynamics of an intramolecular electronic dialogue in porphyrin−C_{60} hybrids. In this paper, we report the synthesis and photophysics of **CuP−C$_{60}$**, a copper-porphyrin−styrene−C_{60} dyad, in which a copper-bound tetraphenylporphine moiety is linked through an alkene unit from one of the pyrrole rings of the porphyrin to the para position of diphenylmethano[60]-fullerene. With the exception of the sp^3-hybridized carbon adjacent to the C_{60}, the system is completely conjugated. The inclusion of copper resulted in the first synthesis of a paramagnetic porphyrin−fullerene dyad, affording a novel material in which the electronically excited donor moiety possesses doublet and quartet spin states in contrast to the singlet and triplet excited states in more familiar types of hybrids incorporating a Zn-porphyrin donor moiety.[1,3,11,17,18] The choice of a paramagnetic copper(II) core in the porphyrin creates a particularly interesting scenario, since augmented electronic coupling with, for example, a fullerene electron-acceptor is expected to enhance the charge-transfer process.

Synthesis

The synthesis of the linker (Scheme 1) was launched from compound **2**, the previously prepared acetal-protected 4-bromomethylbenzophenone.[19] Reaction of **2** with triphenylphosphine affords linker synthon **3**. Copper(II) tetraphenylporphyrinate-2-carboxaldehyde **4** is readily prepared by the previously reported Vilsmeier oxidation of CuTPP.[20] Treatment of **3** with butyllithium (BuLi) generated the ylide required for Wittig coupling with **4** to give **5,** which was shown by ^{1}H NMR to have a trans alkene linkage. Compound **5** is easily deprotected using concentrated HCl in acetone to unmask the benzophenone moiety in *trans*-**6**. Reaction of **6** with *p*-toluenesulfonhydrazide forms a mixture of the syn and anti tosylhydrazones **7**. The mixture was left unresolved for the final step of the synthesis, in which Bamford-Stevens coupling to C_{60} using BuLi afforded

† Part of the special issue "George S. Hammond & Michael Kasha Festschrift".

* Corresponding authors.

‡ Tel: 1-219-631-7441. Fax: 1-219-631-8068. E-mail: Guldi.1@nd.edu.

§ Tel: 1-212-998-8447. Fax: 1-212-260-7905. E-mail: david.schuster@nyu.edu.

10.1021/jp0264836 CCC: $25.00
Published on Web 02/21/2003

SCHEME 1: Preparation of the Copper-Complexed Porphyrin−Fullerene Dyad CuP−C_{60} (1)

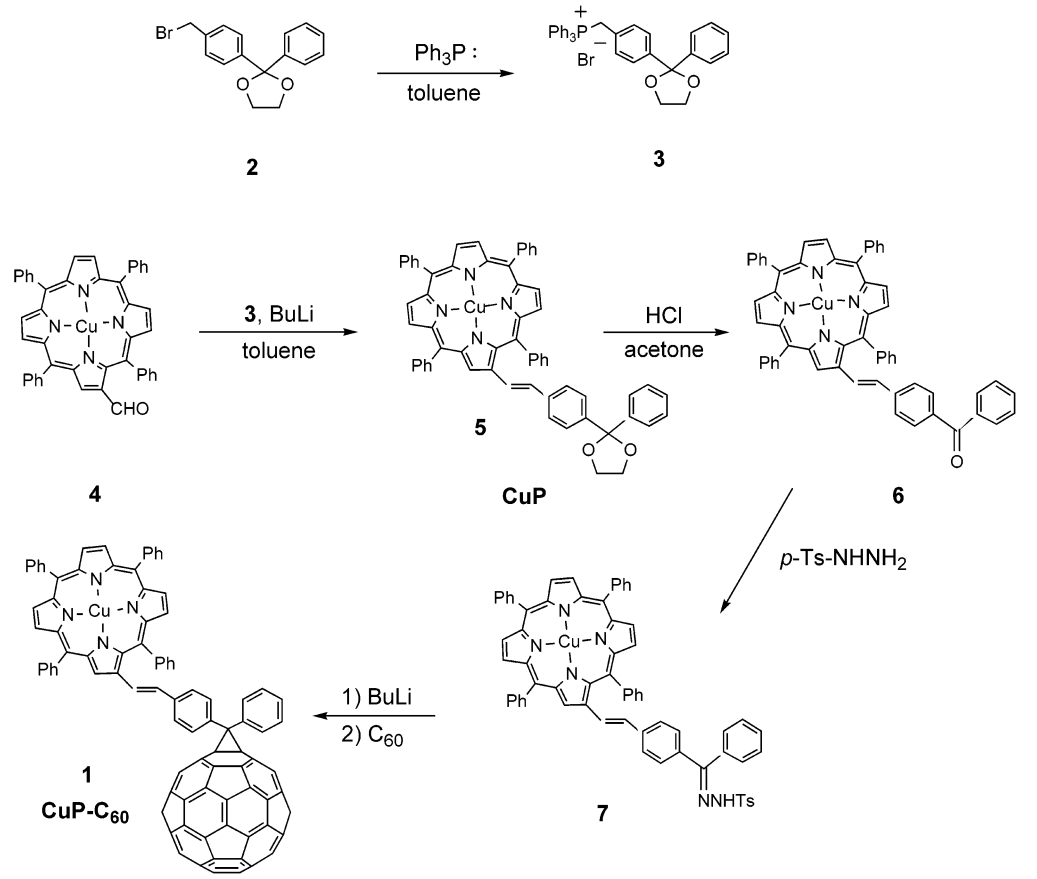

dyad **CuP**−C_{60} (**1**) in 38% yield. The overall yield of the cis/trans mixture of **CuP**−C_{60} from **4** is 11%.

An HPLC chromatogram of the product in the final step revealed the presence of two major bands in a ratio of approximately 9:1. On the basis of TLC and HPLC data for an analogous cis/trans set of fullerostilbenes previously prepared in our laboratory,[21] these peaks were respectively assigned to the *trans*- and *cis*-**CuP**−C_{60} styrene stereoisomers based on their relative chromatographic mobility and the method of synthesis (see spectra in Supporting Information). Thus, while compound **7** was exclusively prepared with *trans*-stereochemistry about the styrene moiety, the harsh conditions of the Bamford-Stevens reaction, i.e., heating in toluene at reflux, partially scrambled the stereochemistry around the double bond. Each of these peaks had marginally faster eluting shoulders, which were attributed to minor amounts of the [5,6]-adducts (versus the more common and stable [6,6]-adducts). Heating the crude mixture of **CuP**−C_{60} in toluene for 2 h at reflux resulted in the disappearance of the shoulders in the chromatogram, an outcome that can be attributed to the rearrangement of the thermodynamically labile [5,6]-adducts to the more stable [6,6]-adducts (see Supporting Information).[22]

The inclusion of the copper within the porphyrin moiety of the dyad resulted in substantial peak broadening in the NMR spectra due to the paramagnetism of the metal. Meaningful ^{13}C NMR data on compounds **4**−**7** could not be obtained. As the majority of the protons in these molecules resonate within the aromatic region, the signals overlapped to form broad, complex multiplets. Since most of the reactions involve the generation or disappearance of one or more nonaromatic functional groups, the ^{1}H NMR spectra, in addition to mass spectra, were still useful for following the reactions and characterizing the compounds produced. The ^{3}He NMR spectrum of dyad **1** synthesized from a doubly enriched sample of $^{3}He@C_{60}$ contained a single peak at −8.0 ppm relative to the signal for gaseous ^{3}He, a typical value for methanofullerene derivatives.[23] The δ −8.0 peak was significantly broader than those typically observed in ^{3}He NMR spectra, presumably due to the presence of the copper atom, so that the presence of both isomers of **1** was masked.

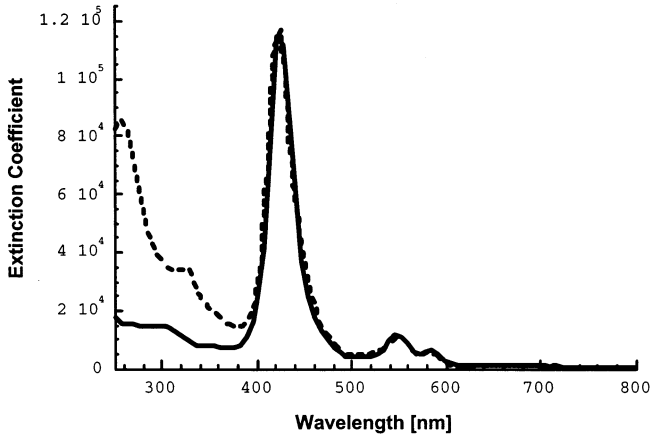

Figure 1. The UV−vis spectra of **CuP**−C_{60} (dashed line) and **CuP** (solid line) in CH_2Cl_2.

The UV−vis electronic absorption spectrum of dyad **1** (**CuP**−C_{60}) in CH_2Cl_2 is shown in Figure 1 along with the spectrum of **CuP** (**5**), both at 10 μM. Electronic interactions between these two redox active moieties should result in lower extinction coefficients and red-shifts in the maxima of the CuP transitions. There is clearly no such change in the dyad spectrum indicative of electronic interactions between the two chromophores in the ground state.

TABLE 1: Electrochemical and Thermodynamic Parameters of CuP−C_{60} in Various Solvents

solvent	$E_{OX}°$ ($D^{+\bullet}$/D) [mV]	$E_{RED}°$ ($A/A^{\bullet-}$) [mV}	$-\Delta G_{CS}°^{b}$ [eV]	$-\Delta G_{CR}°^{b}$ [eV]
toluene[a]			−0.22	1.86
chloroform	160	−1400	0.08	1.56
dichloromethane	490	−1100	0.05	1.59
benzonitrile	460	−1055	0.125	1.515
DMF	530	−860	0.25	1.39

[a] Values could not be obtained in toluene due to immiscibility of the solvent with the TBAP electrolyte. [b] Thermodynamic properties (i.e., $-\Delta G_{CS}°$ and $-\Delta G_{CR}°$) were calculated by applying the dielectric continuum model with reference to the redox potentials measured in chloroform (ϵ= 4.8) and the following parameters: radius_{donor} = 5 Å, $\text{radius}_{acceptor}$ = 4.4 Å, $R_{center-to-center}$ = 16.01 Å, $\epsilon_{toluene}$ = 2.38.[38]

Electrochemistry

An accurate determination of the driving force for the charge-transfer processes (i.e., $-\Delta G_{CS}°$ and $-\Delta G_{CR}°$, see below) necessitates measuring the redox potentials of **CuP−C$_{60}$** and the reference compounds, **CuP** and C_{60}, in the same solvents that were employed for the photochemical experiments. Cyclic voltammetry was performed on solutions of **CuP** and dyad **1** in toluene, chloroform, dichloromethane, *o*-dichlorobenzene, and benzonitrile solutions containing the same supporting electrolyte, 0.1 M *n*-Bu_4NPF_6 (TBAP). The data are summarized in Table 1. Due to the insolubility of the electrolyte in toluene solutions of **1**, it was not possible to obtain viable electrochemical data in this solvent. The first one-electron oxidation potential of **CuP** changes with increasing solvent polarity and, similarly, dyad **1** exhibits positive shifts for the first one-electron reduction potentials of the fullerene core. The driving forces ($-\Delta G_{CR}°$) for intramolecular charge-recombination in **CuP$^{+\bullet}$−C$_{60}^{\bullet-}$** were calculated by eq 1, where *e* stands for the elementary charge:

$$-\Delta G_{CR}° = e[E_{OX}° (D^{+\bullet}/D) - E_{RED}° (A/A^{\bullet-})] \qquad (1)$$

The driving forces for charge-separation ($-\Delta G_{CS}°$) from the photoexcited **CuP** to C_{60} was determined by eq 2:

$$-\Delta G_{CS}° = \Delta E_{0-0} + \Delta G_{CR}° \qquad (2)$$

where ΔE_{0-0} is the excited-state energy of the photoexcited **CuP**. It should be noted that the Coulombic terms in the present donor−acceptor systems are negligible, especially in solvents with moderate or high polarity, because of the relatively long edge-to-edge distance of 8.81 Å and center-to-center distance of 16.01 Å in dyad **1**. Molecular modeling with the Insight II software package[12] (see Experimental) predicts that the plane of the porphyrin extends away from the fullerene moiety (see Figure 2); the rigidity of the styrene linkage prevents the porphyrin from "folding" onto the fullerene cage, as seen in more flexible porphyrin−fullerene hybrids.[5,12]

Photophysical Studies

Emission Spectroscopy. In principle, the weak fluorescence features in copper-based metalloporphyrins[24−26] render emission spectroscopy of **CuP** and **CuP−C$_{60}$** a rather difficult task, especially for probing possible electron or energy transfer processes occurring upon photoexcitation in the Soret- or Q-bands. In a typical room-temperature experiment, **CuP** exhibits no radiative decay in the spectral region between 600 and 900 nm that corresponds to the initially generated singlet−doublet excited state. However, the special photophysical properties of **CuP**, that is, the existence of thermally equilibrated triplet−doublet/triplet−quartet states, analogous to the triplet state of Zn-porphyrins, causes activation of moderately strong and long-lived phosphorescence. Indeed, a broad and structureless emission band centered around 760 nm (1.64 eV) is discernible in frozen toluene matrices as well as in solutions of toluene at room temperature (see Figure 3). The finding that addition of ethyl iodide, an external heavy atom provider, does not change the emission intensity further supports the assignment of the emission to the thermally equilibrated trip-doublet/trip-quartet states.

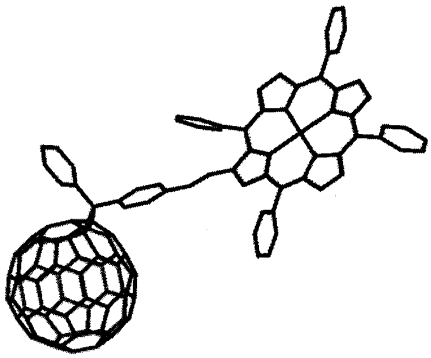

Figure 2. Lowest energy conformation of **CuP−C$_{60}$** as calculated by Insight II.

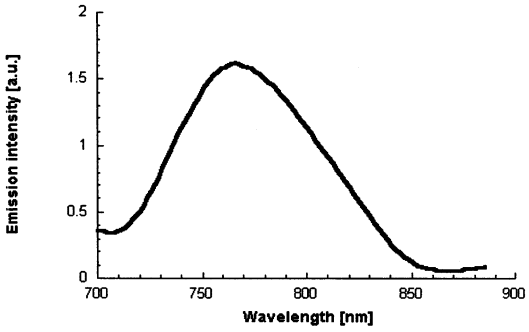

Figure 3. Room-temperature emission spectrum of **CuP** (2.0×10^{-5} M) in toluene; λ_{exc} 580 nm.

Significant quenching of the corresponding emission in the dyad **CuP−C$_{60}$**, after matching the absorption at the **CuP** Q-band transition at 580 nm, was observed. Comparing emission intensity in toluene glasses (at 77 K) or toluene solutions (at 298 K) of **CuP** vs **CuP−C$_{60}$,** we estimate a quenching factor of ∼30. Similar strong quenching was found in benzonitrile, despite the weaker phosphorescence observed in this solvent.[27]

Further support for the emission quenching came from time-resolved measurements. The 760 nm decay of the **CuP** phosphorescence emission in toluene at room temperature is best fitted by a monoexponential decay function, affording lifetimes of 26 ns and 0.6 ns for **CuP** and **CuP−C$_{60}$,** respectively. Shorter lifetimes were observed for **CuP−C$_{60}$** in chloroform (0.31 ns), dichloromethane (0.29 ns), and benzonitrile (0.24 ns).

Transient Absorption Spectroscopy. To complement the fluorescence studies, the photophysics of **CuP** and **CuP−C$_{60}$** were probed by means of time-resolved transient absorption spectroscopy. Short (18 ps) and long (8 ns) laser pulses at 532 nm, which excite the **CuP** chromophore exclusively, allowed for the characterization of the dynamic processes which are associated with the generation and fate of photoexcited states in this novel hybrid.

Differential absorption spectra of **CuP** in an oxygen-free toluene solution reveal the growth of a near-infrared absorption

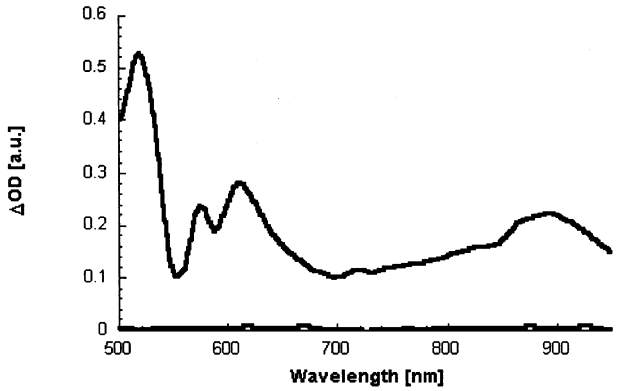

Figure 4. Differential absorption spectra obtained upon picosecond flash photolysis (532 nm) of $\sim 10^{-5}$ M solutions of **CuP** in nitrogen-saturated toluene with a time delay of 0 ps (baseline) and 25 ps (solid spectrum). The lines represent weighted fits of the experimental data points.

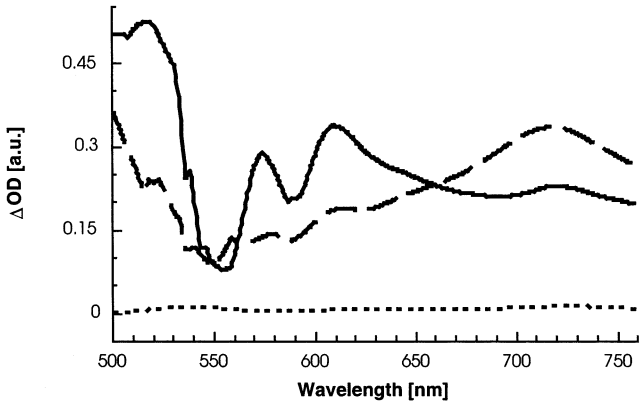

Figure 5. Differential absorption spectra obtained upon picosecond flash photolysis (532 nm) of $\sim 10^{-5}$ M solutions of **CuP**−**C$_{60}$** in nitrogen-saturated toluene with a time delay of 0 ps (dotted spectrum), 25 ps (solid spectrum), and 1000 ps (dashed spectrum). The curves represent weighted fits to the experimental data points.

centered around 880 nm (see Figure 4). Generally, a distinct near-infrared absorption peak in this region is seen in triplet−triplet absorption spectra of tetraphenylporphyrin-based metalloporphyrins, but is not seen in corresponding singlet excited-state absorption spectra.[28] In the visible region, additional maxima at 575, 610, and 720 nm and minima at 540 and 580 nm (corresponding to ground-state bleaching of the **CuP** Q-band transitions) complete the transient characteristics. This is in close agreement with previous observations for several copper-based metalloporphyrins, which exhibit transient absorption originating from the trip-doublet/trip-quartet manifold.[28−30] The grow-in kinetics are buried within the response time of our laser apparatus, namely, 20 ps. Efficient intersystem crossing, induced by the coupling of the paramagnetic d^9-metal center with the normal π-π^* states of porphyrins, is responsible for shortening the singlet−doublet excited-state lifetime to less than 350 fs.[28−30] The resulting **CuP** trip-doublet/trip-quartet state decays by a first-order process.

Similar transient absorption measurements were used to determine the **CuP** trip-doublet/trip-quartet lifetimes in other solvents: chloroform (31 ± 10 ns), dichloromethane (30 ± 10 ns), *o*-dichlorobenzene (30 ± 10 ns), and benzonitrile (33 ± 10 ns).

For the dyad **CuP**−**C$_{60}$**, a broadly absorbing transient was observed in toluene immediately following the 532 nm picosecond laser pulse. A set of distinct maxima at 575, 610, 720, and 880 nm, which characterizes the spectrum of this new species at short time (namely 25 ps after the laser pulse) resembles that seen for **CuP** (see Figure 5). We therefore assign this new transient absorption to the trip-doublet/trip-quartet excited state centered on **CuP**, which evolves by the sequence outlined above. However, in contrast to the 28 ns lifetime for the **CuP**-derived state, the corresponding transient in dyad **1** was much shorter-lived in toluene, decaying with a time constant of 580 ps. The latter is a good match to the value derived from the time-resolved emission decay measurements (vide supra). Furthermore, a new absorption grows in (see Figure 5) with the same time constant (i.e., ∼ 800 ps after the laser pulse), with an absorption maximum at 720 nm, characteristic of fullerene triplet-excited states.[31] We therefore conclude that intramolecular energy transfer has taken place rather than charge separation ($-\Delta G_{CS}°$), which is calculated to be endothermic by 0.22 eV in toluene (see Table 1). Thus, photoexcitation of dyad **CuP**−**C$_{60}$** in toluene initially gives the **CuP**-based trip-doublet/ trip-quartet state (energy 1.64 eV relative to the ground state), which quickly evolves into the triplet excited state localized on C_{60} (1.50 eV).

To determine the decay dynamics of the triplet C_{60} moiety in **CuP**−**C$_{60}$**, we employed an 8 ns laser pulse under conditions similar to those in the picosecond experiments. In general, the nanosecond and picosecond results are in excellent agreement with each other, disclosing strong typical C_{60}-based triplet−triplet absorption at 720 nm. A clean monoexponential recovery of the singlet ground state follows at low substrate concentration and low laser power, corresponding to a fullerene triplet lifetime of nearly 20 μs. Under our standard conditions, triplet lifetimes of fullerene derivatives are typically on the order of 20 μs.[31] The triplet quantum yield in toluene was determined from the absorption at 720 nm to be 0.34.

The failure to observe charge-separation on photoexcitation of **CuP**−**C$_{60}$** in toluene led us to run analogous picosecond and nanosecond experiments in benzonitrile, a much more polar solvent. Immediately following the laser pulse, we observed exactly the same **CuP** trip-doublet/trip-quartet spectral features described above for toluene, namely absorption maxima at 575, 610, 720, and 880 nm (see Figure 5), and Q-band bleaching at 580 nm. It is interesting to note that in coordinating solvents, including benzonitrile, square planar tetracoordinated **CuP** transforms into a pentacoordinated analogue with pyramidal geometry. This relatively dramatic structural alteration is accompanied by a red-shift of the Soret- and Q-band transitions by about 15 nm. Thus, our picosecond results in benzonitrile suggest excitation of the pentacoordinated **CuP** in **CuP**−**C$_{60}$**.[32] As shown in Figure 6, appreciable acceleration of the **CuP** trip-doublet/trip-quartet decay occurrs in benzonitrile, with a time constant of 299 ps, to give a broadly absorbing species, as seen in Figure 7, that is spectrally distinct from the C_{60} triplet state and **CuP** ground state. The maximum at 660 nm is ascribed to the ligand-centered one-electron oxidized form of the donor, **CuP**$^{+\bullet}$, while the maximum in the near-infrared region at 1040 nm is an excellent match to the one-electron reduced methanofullerene, $C_{60}^{\bullet-}$.[31] We therefore conclude that in benzonitrile, **CuP**$^{+\bullet}$−**C$_{60}^{\bullet-}$** is formed via the **CuP** trip-doublet/trip-quartet excited state with an overall quantum yield of ∼0.10.

Extending our experiments into the nanosecond domain, we were able to determine the lifetime of the **CuP**$^{+\bullet}$−**C$_{60}^{\bullet-}$** charge-separated state. Using nitrogen-purged solutions, both fingerprints, namely, decay of **CuP**$^{+\bullet}$ absorption at 660 nm and decay of $C_{60}^{\bullet-}$ absorption at 1040 nm, reveal a decay time constant of 140 ± 10 ns. To correlate this observation with the Marcus

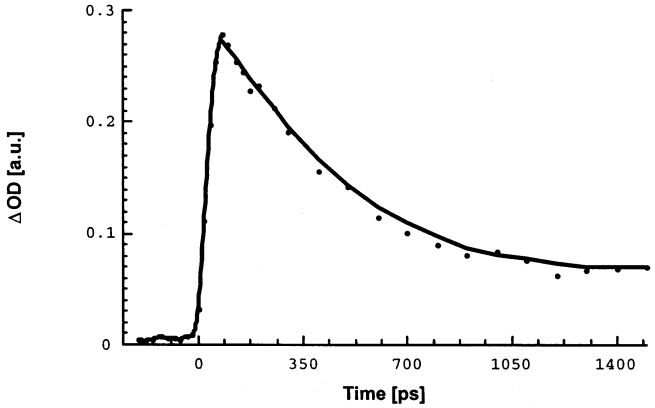

Figure 6. Time-absorption profile at 720 nm, displaying the initial formation of the photoexcited **CuP** chromophore in **CuP**−$\mathbf{C_{60}}$ and its subsequent decay. The curve shown is the best fit to the decay data.

TABLE 2: Photophysical Parameters of CuP−C_{60} in Various Solvents

solvent	dielectric constant	CuP−C_{60} rate of charge separation	CuP−C_{60} rate of charge recombination	Φ_{CS}
toluene	2.38	1.7×10^9 s^{-1} *a,b,c*		0.34 *d*
chloroform	4.8	3.2×10^9 s^{-1} *e*	2.4×10^6 s^{-1}	0.18
dichloromethane	9.08	3.4×10^9 s^{-1} *e*	2.7×10^6 s^{-1}	0.25
o-dichlorobenzene	9.98	not measured	2.9×10^6 s^{-1}	0.21
benzonitrile	24.8	3.5×10^9 s^{-1} *b,f*	7.1×10^6 s^{-1}	0.10

a Energy transfer. *b* From transient absorption measurements. *c* 0.6 ns − from time-resolved emission decay measurements. *d* Quantum yield for the fullerene triplet; no ET observed. *e* From time-resolved emission decay measurements. *f* Compare to 0.24 ns from time-resolved emission decay measurements

theory of electron transfer and to explore the question of solvent stabilization of the charge-separated state in this paramagnetic system, we measured the lifetime of the **CuP**$^{+\bullet}$−$\mathbf{C_{60}}^{\bullet-}$ radical pair in solvents of varying polarity, namely chloroform, dichloromethane, and *o*-dichlorobenzene (see Table 2). From the free energies for charge recombination, $-\Delta G_{CR}°$ (see Table 1), we conclude that the charge-recombination dynamics in **CuP**$^{+\bullet}$−$\mathbf{C_{60}}^{\bullet-}$ are located in the inverted region of the Marcus curve, where the rate constants decrease as the thermodynamic driving force for back electron transfer increases.[1,5,33,34] The reorganization energies (λ) for metalloporphyrin−fullerene dyads typically range between 0.6 and 0.8 eV.[5,31,33−35] We calculated the solvent reorganization energies (λ_S) for **CuP**−$\mathbf{C_{60}}$ in *o*-dichlorobenzene and benzonitrile, which are 0.73 and 0.88 eV, respectively. In a first-order approximation, we treat the internal reorganization energy (λ_I) of **CuP** and $\mathbf{C_{60}}$ as constant, in accord with closely related earlier studies.[33,36]

Conclusions

In summary, the present study demonstrates that in this **CuP**−$\mathbf{C_{60}}$ donor−acceptor dyad possessing a styrene linker, the paramagnetic copper(II) core augments the electronic coupling with the electron accepting fullerene and, in turn, influences the charge-transfer process. The photophysical dynamics observed following irradiation of **CuP**−$\mathbf{C_{60}}$ in nonpolar *vs* polar solvents are summarized in Figure 8. The basic reactivity of photoexcited **CuP**−$\mathbf{C_{60}}$, that is, triplet−triplet energy transfer in toluene and electron transfer in polar solvents, both evolving from the photoexcited metalloporphyrin, resembles earlier findings with a ruthenium(II)-based tetraphenylporphyrin, **RuP**.[37] As a reference point, lifetimes shorter than 4 ns were reported for **RuP**$^{+\bullet}$−$\mathbf{C_{60}}^{\bullet-}$. Since the donor−acceptor separation is much greater (8.81 Å edge-to-edge, 16.01 Å center-to-center) in the case of **CuP**−$\mathbf{C_{60}}$ compared with the **RuP**−$\mathbf{C_{60}}$ hybrid,[37] it is not surprising that the lifetime of the **CuP**$^{+\bullet}$−$\mathbf{C_{60}}^{\bullet-}$ state is enhanced, up to 415 ± 30 ns (in chloroform). The suggestion that this is due to the generation of Cu(III) by a second electron-transfer step from Cu(II) to the porphyrin radical cation was rejected on the basis of the unfavorable free energy change associated with such a process. Furthermore, the presence of an unpaired electron on the metal center renders **CuP**-based donor−acceptor dyads particularly interesting as spin probes. Experiments along these lines are currently in progress.

Experimental

Photophysical Studies. Picosecond laser flash photolysis experiments were carried out with 532-nm laser pulses from a

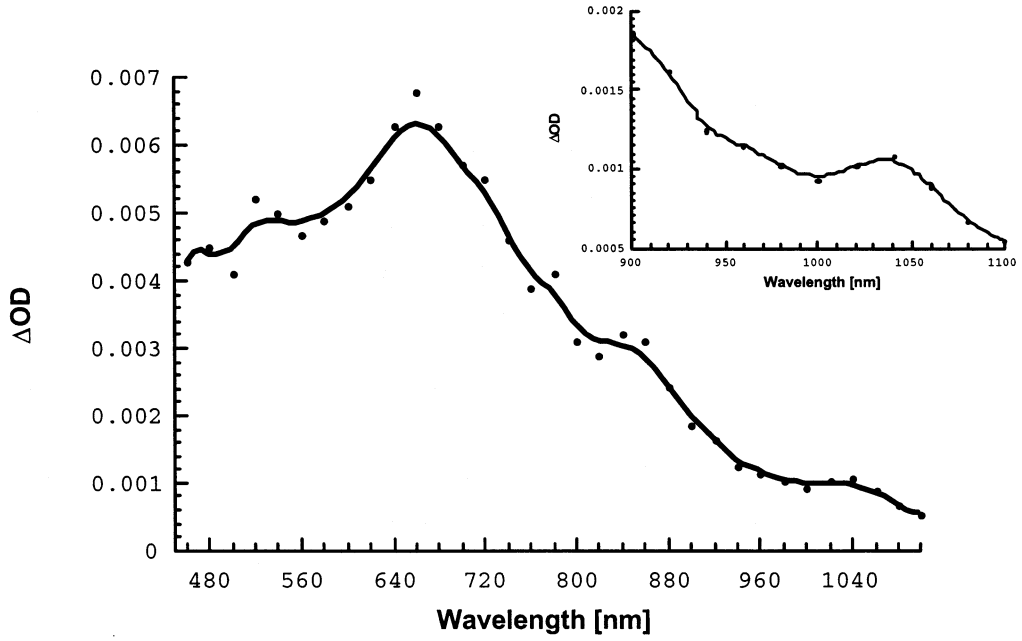

Figure 7. Differential absorption spectra obtained after 50 ns upon nanosecond flash photolysis (532 nm) of ~10^{-5} M solutions of **CuP**−$\mathbf{C_{60}}$ dyad in deoxygenated benzonitrile. The insert shows a magnification of the spectrum in the near-infrared region, showing absorption at 1040 nm attributed to the C_{60} radical anion. The curves represent weighted fits to the experimental data points.

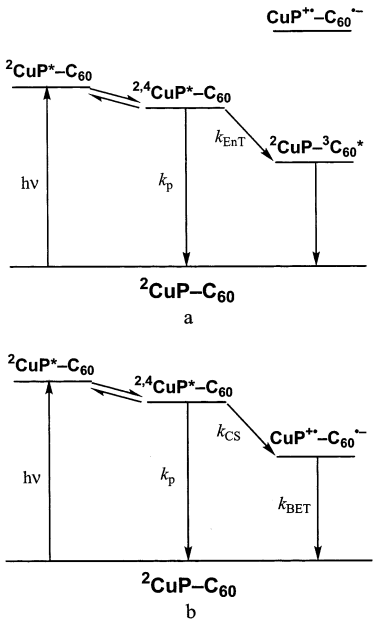

Figure 8. Jablonski diagrams summarizing the photophysical pathways observed following irradiation of dyad **1** in (a) toluene and (b) chloroform, CH_2Cl_2, *o*-DCB, and DMF. The energy levels shown represent relative, not absolute, energies.

mode-locked, Q-switched Quantel YG-501 DP Nd:YAG laser system (pulse width 18 ps, 2−3 mJ/pulse). Nanosecond laser flash photolysis experiments were performed with laser pulses from a Quanta-Ray CDR Nd:YAG system (532 nm, 6 ns pulse width) in a front face excitation geometry. The photomultiplier output was digitized with a Tektronix 7912 AD programmable digitizer. Fluorescence lifetimes were measured with a Laser Strope Fluorescence Lifetime Spectrometer (Photon Technology International) with 337 nm laser pulses from a nitrogen laser fiber-coupled to a lens-based T-formal sample compartment equipped with a stroboscopic detector. Details of the laser strobe systems are described on the manufacturer's web site, http://www.pti-nj.com. Emission spectra were recorded with an SLM 8100 spectrofluorometer. The experiments were performed at room temperature. A 570 nm long-pass filter in the emission path was used in order to eliminate the interference from the solvent and stray light for recording the fullerene fluorescence. Each spectrum was an average of at least five individual scans and was corrected by using the correction function supplied by the manufacturer, by subtraction of the photomultiplier dark counts signal.

Electrochemistry. Electrochemical studies were carried out using an AFRDE4 Bi-potentiostat. Cyclic voltammograms were recorded at a scan rate of 100 mV/s in a conventional three-electrode system. A Glassic carbon electrode was used as the working electrode, a silver electrode as the reference electrode, and a platinum wire served as the counter electrode. All potentials were referenced to an internal ferrocene/ferrocenium redox couple. All solutions were also purged with argon gas prior to spectral and electrochemical measurements. Experiments were run under atmospheric temperature and pressure using 0.1 M concentrations of the TBAP electrolyte.

Molecular Modeling. The copper porphyrin−fullerene dyad (**CuP−C$_{60}$**) was constructed and investigated using the Insight II version 2000 software package (Accelrys Inc., San Diego, CA). See ref 12 for details of the method. The ESFF (Extensible Systematic Force field) was employed as it incorporates parameters for transition metals into its atom type set and is thus particularly well suited for computations on metalloporphyrin derivatives. Once the force field was chosen, minimum energy functions were applied to calculate the bond lengths and angles based on steric and electronic considerations. The distance from the center of the fullerene to the copper atom was found to be 16.01 Å, while the edge-to-edge distance (the shortest distance from a carbon atom on the fullerene cage to the closest atom on the central porphyrin ring) was calculated to be 8.81 Å.

Synthesis

All chemicals were purchased from Aldrich Chemical Co. (Milwaukee, WI) or Lancaster Synthesis (Windham, NH) and were used without further purification. NMR spectra for 200 and 300 MHz measurements were acquired on Varian Gemini spectrometers. Matrix-Assisted Laser Desorption/Ionization Time-of-Flight (MALDI-TOF) mass spectra were recorded on a Kratos Kompact model, manufactured by Shimadzu Scientific Instruments.

Linker 3. A sample of bromide **2**[19] (2.67 g, 8.69 mmol) was dissolved in 20 mL of anhydrous toluene under nitrogen. The solution was cooled in an ice−water bath and triphenylphosphine (2.19 g, 8.35 mmol) was added. A white precipitate of **3** formed immediately and the mixture was heated at reflux for 48 h. The white precipitate was isolated by suction filtration, washed with hot benzene, and dried. The yield of **3** was 3.52 g (6.07 mmol, 73%).

***p*-(Cu-5,10,15,20-tetraphenylporphyrin-3-*trans*-ethenyl)-benzophenone ketal 5.** Under a nitrogen atmosphere, synthon **3** (150.7 mg, 260 μmol) was dissolved in 35 mL of anhydrous benzene. A 162 μL (259 μmol) aliquot of a 1.6 M solution of butyllithium in hexanes was injected and the mixture was stirred for 3 h. A solution of porphyrin−carboxaldehyde **4**[20] (182.5 mg, 259 μmol) in 100 mL of dry benzene was transferred to the original flask and the solution was heated at reflux for 17 h. The cool reaction mixture was extracted with 100 mL of water and the solvent was removed by rotary evaporation. The residue was redissolved in a minimal amount of CH_2Cl_2 and the desired product was isolated by flash chromatography (SiO_2 w/CH_2Cl_2). The desired product **5** was in the first eluted fraction.

^{1}H NMR ($CDCl_3$, 200 MHz): δ 8.8 (s), 8.2 (s, br), 6.7−8.1 (m, br), 5.3 (d), 4.1 (t), 0.5−2.1 (br, m). UV−Vis (C_6H_{12}): 422 nm (241,000), 547 nm (22,300), 582 nm (9940). MALDI-TOF MS ($C_{61}H_{42}CuN_4O_2$): *m*/*z* calcd for MH^+, 929; found. 926.

***p*-(Cu-5,10,15,20-tetraphenylporphyrin-3-*trans*-ethenyl)-benzophenone 6.** A sample of **5** was dissolved in a mixture of 10 mL CH_2Cl_2 and 250 mL of acetone. A 3 mL aliquot of concentrated HCl was added and the solution was stirred for 90 min at room temperature. The solvent was removed by rotary evaporation and the residue redissolved in a minimal amount (~25 mL) of CH_2Cl_2. This solution was extracted three times with a saturated aqueous solution of $NaHCO_3$. The organic layer was dried over Na_2SO_4 and evaporated to yield compound **6** (131 mg, 148 μmol). The combined yield of the last two steps (conversion of **4** to **6**) was 57%.

^{1}H NMR ($CDCl_3$, 200 MHz): δ 6.7−8.4 (m, br), 5.3 (s), 2.2 (s), 1.6 (br, s), 1.3 (br, s), 0.8 (br, s). IR: 3440 cm^{-1} (br), 1653 cm^{-1} (s). MALDI-TOF MS ($C_{59}H_{38}CuN_4O$): *m*/*z* calcd for MH^+, 882; found, 886.

Tosylhydrazones 7. In a short-path distillation apparatus under a nitrogen atmosphere, compound **6** (18.4 mg, 20.8 μmol) and *p*-toluenesulfonhydrazide (7.1 mg, 38 μmol) were dissolved in 25 mL of anhydrous benzene and the solution was heated at reflux with an external oil bath. The temperature was regulated (~140 °C) such that the solvent slowly distilled until only a

few drops remained. These last remnants of solvent were removed in vacuo and the *p*-toluenesulfonhydrazone was isolated by flash chromatography (SiO_2 w/$CHCl_3$). HPLC analysis suggests compound **7** (15.5 mg, 14.8 μmol, 71%) was obtained as a mixture of cis- and trans- hydrazone isomers, which was used directly for the synthesis of dyad **1**.

^{1}H NMR ($CDCl_3$, 200 MHz): δ 6.6−8.4 (m), 5.3 (s), 2.4 (t), 1.3 (br, s), 0.9 (br, s).

CuP−C_{60} Dyad 1. In a small Dean−Stark apparatus under an atmosphere of nitrogen, a 45.2 mg (43.0 μmol) portion of **7** was dissolved in 60 mL of anhydrous toluene and deprotonated by the addition of 25.1 μL (40.2 μmol) of 1.6 M BuLi in hexanes. A solution of C_{60} (37 mg, 51 μmol) in 50 mL of anhydrous toluene was transferred to the still and the mixture was heated at reflux for 50 min. The solvent was then allowed to drain from the trap until only a few drops remained in the still portion, and the last remnants of solvent were removed in vacuo. The yield dropped significantly in trials where the solvent was not completely removed. The residue was dissolved in a minimal amount of CS_2. The cis and trans isomers of **1** were resolved by preparative TLC (SiO_2 w/CS_2). HPLC analysis suggested a minor amount of [5,6]-adducts in addition to the [6,6]-isomers. Consistent with this hypothesis, heating the crude mixtures of adducts for 2 h at reflux in toluene led to disappearance of these extraneous HPLC peaks, leaving only pure *cis*- and *trans*-**1**, consistent with conversion of the [5,6] adducts to their more stable [6,6] isomers. The total yield of dyad **1** was 26 mg (16 μmol, 38%).

^{1}H NMR: A meaningful ^{1}H NMR spectrum could not be obtained. ^{3}He NMR (400 MHz): δ −8.0 (br, s). UV−Vis (C_6H_{12}): 258 nm (23,300), 327 nm (9,770), 424 nm (36,400), 547 nm (3,900), 582 nm (2,100). FAB$^+$ MS ($C_{119}H_{38}CuN_4$): *m*/*z* calcd. for M^+, 1585.3; found, 1586.4.

Acknowledgment. We thank Dr. Chuping Luo for preliminary photophysical studies on these materials. We are grateful to Prof. Martin Saunders and Dr. Anthony Khong for the sample of ^{3}He@C_{60} and for the ^{3}He NMR spectrum of dyad **1**. FAB mass spectral data were obtained at the Michigan State University Mass Spectrometry Facility which is supported, in part, by a grant (DRR-00480) from the Biotechnology Research Technology Program, National Center for Research Resources, National Institutes of Health. This work was funded by the NSF (CHE-9712735), the NYU College of Arts and Science (Morse Grant to P.J.B.), the Arnold and Mabel Beckman Foundation (Beckman Scholars Program Award to P.J.B.), and the U.S. Office of Basic Energy Sciences of the Department of Energy. This is document NDRL-4431 from the Notre Dame Radiation Laboratory.

Supporting Information Available: HPLC chromatograms of a ∼1:2 mixture of *cis*- and *trans*-fullerostilbenes (Figure S1), of the **CuP−C_{60}** dyad **1** as isolated from the Bamford Stevens reaction (Figure S2), and of dyad **1** after being heated for 2 h in refluxing toluene (Figure S3); UV-vis spectrum of dyad **1** (Figure S4), ^{3}He NMR spectrum of ^{3}He@dyad **1** (Figure S5), ^{1}H NMR spectrum of tosylhydrazone **7** (Figure S6), and UV-Vis spectrum of **CuP** (reference compound **5**) (Figure S7). This material is available free of charge via the Internet at http://pubs.acs.org.

References and Notes

(1) (a) Guldi, D. M. *Chem. Commun.* **2000**, 321. (b) Guldi, D. M. The Small Reorganization Energy of Fullerenes. In *Fullerenes*: *From Synthesis to Optoelectronic Properties*; Guldi, D. M., Martin, N., Eds.; Kluwer Academic Publishers: Norwell, MA, 2002; p 237.

(2) Martín, N.; Sánchez, L.; Illescas, B.; Pérez, I. *Chem. Rev.* **1998**, *98*, 2527.

(3) Guldi, D. M.; Kamat, P. V. Photophysical Properties of Pristine Fullerenes, and Fullerene-Containing Donor-Bridge-Acceptor Systems. In *Fullerenes: Chemistry, Physics, and Technology*; Kadish, K. M., Ruoff, R. S., Eds.; John Wiley and Sons: New York, 2000; p 225.

(4) Schuster, D. I. *Carbon* **2000**, *38*, 1607.

(5) Bracher, P. J.; Schuster, D. I. Electron Transfer in Functionalized Fullerenes. In *Fullerenes: From Synthesis to Optoelectronic Properties*; Guldi, D. M., Martin, N., Eds.; Kluwer Academic Publishers: Norwell, MA; 2002, p 163.

(6) Imahori, H.; Sakata, Y. *Adv. Mater.* **1997**, *9*, 537.

(7) Gust, D.; Moore, T. A.; Moore, A. L. *Acc. Chem. Res.* **2001**, *34*, 40.

(8) Reed, C. A.; Bolskar, R. D. *Chem. Rev.* **2000**, *100*, 1075.

(9) Diederich, F.; Gomez-Lopez, M. *Chem. Soc. Rev.* **1999**, *28*, 263.

(10) Prato, M. *J. Mater. Chem.* **1997**, *7*, 1097.

(11) Kuciauskas, D.; Lin, S.; Seely, G. R.; Moore, A. L.; Moore, T. A.; Gust, D.; Drovetskaya, T.; Reed, C. A.; Boyd, P. D. W. *J. Phys. Chem.* **1996**, *100*, 15926.

(12) Schuster, D. I.; Jarowski, P. D.; Kirschner, A. N.; Wilson, S. R. *J. Mater. Chem.* **2002**, *12*, 2041.

(13) Schuster, D. I.; Cheng, P.; Wilson, S. R.; Prokhorenko, V.; Katterle, M.; Holzwarth, A. R.; Braslavsky, S. E.; Klihm, G.; Williams, R. M.; Luo, C. *J. Am. Chem. Soc.* **1999**, *121*, 11599.

(14) Guldi, D. M.; Luo, C.; Prato, M.; Dietel, E.; Hirsch, A. *Chem. Commun.* **2000**, 373.

(15) Armaroli, N.; Marconi, G.; Echegoyen, L.; Bourgeois, J.-P.; Diederich, F. *Chem. Eur. J.* **2000**, *6*, 1629.

(16) Armaroli, N. Photoinduced Energy Transfer Processes in Functionalized Fullerenes. In *Fullerenes*: *From Synthesis to Optoelectronic Properties*; Guldi, D. M., Martin, N., Eds.; Kluwer Academic Publishers: Norwell, MA, 2002; p 137.

(17) Liddell, P. A.; Sumida, J. P.; MacPherson, A. N.; Noss, L.; Seely, G. R.; Clark, K. N.; Moore, A. L.; Moore, T. A.; Gust, D. *Photochem. Photobiol.* **1994**, *60*, 537.

(18) Imahori, H.; Hagiwara, K.; Aoki, M.; Akiyama, T.; Taniguchi, S.; Okada, T.; Shirakawa, M.; Sakata, Y. *J. Am. Chem. Soc.* **1996**, *118*, 11771.

(19) Masuhara, H.; Maeda, Y.; Nakajo, H.; Mataga, N.; Tomita, K.; Tatemitsu, H.; Sakata, Y.; Misumi, S. *J. Am. Chem. Soc.* **1981**, *103*, 634.

(20) Binstead, R. A.; Crossley, M. J.; Hush, N. S. *Inorg. Chem.* **1991**, *30*, 1259.

(21) (a) Nuber, B.; Khong, A.; Wilson, S. R.; Schuster, D. I. *Proc. Electrochem. Soc.* **2000**, *9*, 161. (b) Schuster, D. I.; Nuber, B.; Vail, S. A.; MacMahon, S.; Lin, C.; Wilson, S. R.; Khong, A. *Photochem. Photobiol. Sci.* **2003**, in press.

(22) Wilson, S. R.; Schuster, D. I.; Nuber, B.; Meier, M. S.; Maggini, M.; Prato, M.; Taylor, R. Organic Chemistry of Fullerenes. In *Fullerenes: Chemistry, Physics, and Technology*; Kadish, K. M., Ruoff, R. S., Eds.; John Wiley and Sons: New York, 2000; p 91.

(23) Saunders: M.; Cross, R. J.; Jimenez-Vazquez, H. A.; Shimshi, R.; Khong, A. *Science* **1996**, *271*, 1693.

(24) Smith, B. E.; Gouterman, M. *Chem. Phys. Lett.* **1968**, *2*, 517.

(25) Asano-Someda, M.; Sato, S.-I.; Aoyagi, K.; Kitagawa, T. *J. Phys. Chem.* **1995**, *99*, 13800.

(26) Asano-Someda, M.; Kaizu, Y. *Photochem. Photobiol. A* **1995**, *87*, 23.

(27) It is well-known that chelation of the axial position of CuP with pyridine, benzonitrile, and other σ-donor ligands causes out-of-plane structural distortion, which mainly dictates the excited-state structure and dynamics. See Kim, D.; Holten, D.; Gouterman, M. *J. Am. Chem. Soc.* **1984**, *106*, 2793−2798.

(28) Rodriguez, J.; Kirmaier, C.; Holten, D. *J. Am. Chem. Soc.* **1989**, *111*, 6500.

(29) Yan, X.; Holten, D. *J. Phys. Chem.* **1988**, *92*, 5982.

(30) LeCours, S. M.; Philips, C. M.; Paula, J. C. d.; Therien, M. J. *J. Am. Chem. Soc.* **1997**, *119*, 12578.

(31) Guldi, D. M.; Prato, M. *Acc. Chem. Res.* **2000**, *33*, 695.

(32) A similar conclusion was reached in recent transient absorption measurements.

(33) Imahori, H.; Tamaki, K.; Guldi, D. M.; Luo, C.; Fujitsuka, M.; Ito, O.; Sakata, Y.; Fukuzumi, S. *J. Am. Chem. Soc.* **2001**, *123*, 2607.

(34) Imahori, H.; Sakata, Y. *Eur. J. Org. Chem.* **1999**, 2445.

(35) Guldi, D. M. *Chem. Soc. Rev.* **2002**, *31*, 22.

(36) Osuka, A.; Noya, G.; Taniguchi, S.; Okada, T.; Nishimura, Y.; Yamazaki, I.; Mataga, N. *Chem. Eur. J.* **2000**, *6*, 33.

(37) Da Ros, T.; Prato, M.; Guldi, D. M.; Ruzzi, M.; Pasimeni, L. *Chem. Eur. J.* **2001**, *7*, 816.

(38) Imahori, H.; Hagiwara, K.; Aoki, M.; Akiyama, T.; Taniguchi, S.; Okada, T.; Shirakawa, M.; Sakata, Y. *J. Am. Chem. Soc.* **1996**, *118*, 11771.